Hindawi
Advances in Civil Engineering
Volume 2022, Article ID 7954991, 13 pages
https://doi.org/10.1155/2022/7954991

Research Article

Study on Stability Reduction Characteristics of Earth and Rockfill Dams under Rapid Drawdown Using Fully Coupled Seepage-Stress Analysis

Yong Nam Ri,[1] Un Chol Han ,[2] Ui Jun Jang,[1] Dok Yong Jong,[1] and Chol Ung Kim[1]

[1]*Faculty of Geological Prospecting Engineering, Kim Chaek University of Technology, Pyongyang 999093, Democratic People's Republic of Korea*
[2]*School of Science and Engineering, Kim Chaek University of Technology, Pyongyang 999093, Democratic People's Republic of Korea*

Correspondence should be addressed to Un Chol Han; huch8272@star-co.net.kp

Received 22 July 2021; Revised 8 November 2021; Accepted 21 December 2021; Published 22 January 2022

Academic Editor: Minghui Li

It can be a great expense to examine individually the stability of earth and rockfill dams on rapid drawdown in civil engineering practice. The aim of this present work is to clarify the safe type on the rapid drawdown among the most common types of earth and rockfill dams and to introduce cheaply the types in dam design. First, a transient analysis of saturated-unsaturated seepage coupled with stress is carried out in the cross sections of typical earth and rockfill dams the during rapid drawdown, and the safety factors of the upstream slopes are determined by the shear strength reduction method. Then, the typical dams are compared for the stability characteristics so that designers can select the safe type of earth and rockfill dams on rapid drawdown. The obtained results show that the decreasing rate of safety factor in a central core dam is 0.72–0.85 times than one of the homogeneous dams and 0.17–0.40 times than one of the sloping upstream core dams so that it is more stable than other earth and rockfill dams during rapid drawdown.

1. Introduction

The stability of earth and rockfill dams (ERDs) includes usually the sliding stabilities of steady seepage (at levels of normal water or flood water), earthquake, and transient seepage (drawdown or heading up). The phreatic surface, shear strength, boundary condition, and effective stress of the slope soil are dynamically changed, and there are coupled seepage stress and nonlinear characteristics in transient seepage such as rapid drawdown (RDD) unlike steady seepage. Therefore, there are a few difficulties in evaluating the stability for transient seepage. For this reason, it is expensive and not effective to evaluate individually the stability on RDD at the stage of designing in which a designer chooses a type of dam.

The ERDs frequently met in civil engineering practice can be classified into a homogeneous, sloping upstream core, and central core according to whether they have an impervious core or not and where the impervious core exists. If a designer knows the stability reduction characteristics of the typical ERDs and has the knowledge of dam type that is more stable on RDD before beginning the design of dams, it allows the designer to design the safer ERD at a low calculation cost.

There are some investigations to evaluate the stability of slope under RDD by using saturated-unsaturated seepage analysis, coupled seepage-stress analysis, and the shear strength reduction finite element method (FEM). Some literature studies have numerically studied the effects of the drawdown rate, drawdown ratio, and permeability of slope soil on the slope stability during RDD. The drawdown rate is the drawdown drop per unit time, and the drawdown ratio is defined as the ratio of the total drawdown drop to the initial water head.

Huang and Jia [1] evaluated the stability of the homogeneous dam under RDD by using the transient analysis of unsaturated seepage and FEM with a shear strength reduction technique and presented the stability variation characteristics of the homogeneous dam during RDD, while Berilgen [2] studied the slope stability during drawdown depending on the soil permeability, drawdown rate, and drawdown ratio with considering the nonlinear material and loading conditions. Also, Khanna et al. [3] analyzed the stability of the central core dam of 180m height to show that the safety factor of the upstream slope under RDD remains high when the thickness of the vertical core is less than 150% of the height of the dam, and Boushehrian et al. [4] presented that the horizontal drains in the upstream slope of the dams increase the safety factor of the upstream slope up to 24% for homogeneous dams and 17% for heterogeneous dams.

Besides, Tsiampousi et al. [5] investigated the relationship between the safety factor and time for an excavation performed in an unsaturated silt soil using FEM and demonstrated that, for unsaturated soils, the safety factor may increase with time, in contrast to what is commonly accepted to be the case in fully saturated soils. They examined parametrically the effects of which unsaturated soil permeability, its variation with suction, the increase of apparent cohesion due to suction, the depth of the groundwater table, and the hydraulic hysteresis have on the results of the unsaturated analysis.

Meanwhile, Pinyol et al. [6] compared the predictions of four calculation procedures with pore pressure records measured in Glen Shira dam during a controlled drawdown and presented that only the coupled analysis provides a consistent and reasonable solution, and Chen and Huang [7] presented that the strength reduction method used in FEM is very effective in capturing the progressive failure induced by reservoir water level fluctuations. Also, Stark and Jafari [8] showed that unsaturated and transient seepage analyses can be used to evaluate the progression of the phreatic surface through the fine-grained core and estimate the seepage induced, not shear induced, pore water pressures during drawdown through the stability analyses of San Luis dam. Keykhah and Zadeh [9] analyzed the stability of the upstream slope of Ilam dam against a sudden change in the water level of the reservoir to overcome the existing shortcomings of FEMs.

To the best of our knowledge, there seem to be no studies regarding which type of ERD is safe for RDD.

This work aims to compare the variation characteristics of sliding stability for typical ERDs during RDD with the same drawdown rate, drawdown ratio, and soil permeability, and to allow a designer to reduce the calculation cost by selecting the safe type on RDD among the typical ERDs in civil engineering practice.

The present work compares the sliding stability reduction characteristics of typical ERDs under relatively "slow" drawdown and "rapid" drawdown, "high" drawdown ratio and "low" drawdown ratios. For this purpose, it is assumed that saturated-unsaturated transient seepage occurs in ERDs, and the shear strength of soils in the unsaturated zone is a function of the degree of saturation. And it uses a finite element analysis of coupled transient seepage and deformation with shear strength reduction technique and a relationship curve between horizontal displacement and reduction factor in order to obtain the safety factor of dams. The obtained results will be useful to overcome the sliding failure of ERDs induced by an operational drawdown in civil engineering practice. It also allows designers to reduce the calculation cost for selecting the safe type of ERDs on RDD.

2. Stress Equilibrium in Unsaturated Soils

Unsaturated soil is a multiphase material composed of soil particles, water, and air. Therefore, the presence of two fluids in the medium should be considered in the modeling of unsaturated soils with the soil skeleton.

It can be assumed that water is relatively incompressible and air is relatively compressible in unsaturated soils. According to the effective stress principle, the total stress acting at a point, σ, is made up of an average pressure stress in the pore water, u_w, which is called the "wetting liquid pressure," an average pressure stress in the pore air, u_a, and an "effective stress," σ'.

$$\sigma' = \boldsymbol{\sigma} + (\chi u_w + (1 - \chi)u_a)\mathbf{I}, \tag{1}$$

where χ is a factor that depends on the degree of saturation and the surface tension of the liquid-solid system [10]. χ is 1.0 in saturated soils and ranges from 0.0 to 1.0 in unsaturated soils because it depends on the degree of saturation of the medium. In order to simplify, it can be assumed that χ is equal to the degree of saturation of the medium. $\mathbf{I}$ is the unit matrix.

It is adopted by the following assumptions:

(i) The air (the nonwetting fluid) in unsaturated soils can diffuse through the medium freely

(ii) The air in unsaturated soils is exposed to the atmosphere

(iii) The gravitational gradient of atmospheric pressure cannot cause a significant variation in the air pressure, and there can be no external event that provides a transient variation in the air pressure

These assumptions allow the above equation to express simply as follows:

$$\sigma' = \boldsymbol{\sigma} + \chi u_w \mathbf{I}. \tag{2}$$

In the case that trapped fluid exists in the medium, the effective stress is assumed as follows:

$$\sigma' = (1 - n_t)\overline{\sigma} - n_t \overline{p}_t \mathbf{I}, \tag{3}$$

where $\overline{\sigma}$ is the effective stress in the skeleton of the porous material, $\overline{p}_t$ is the average pressure stress in the trapped liquid, and n_t is the ratio of trapped fluid volume to total volume.

Stress equilibrium for the solid can be expressed from the principle of virtual work. For a small element at the time of t, the principle of virtual work can be represented as follows:

$$\int_V (\sigma' - \chi u_w \mathbf{I}) \cdot \delta\boldsymbol{\varepsilon} dV = \int_F \mathbf{R}_F \cdot \delta\mathbf{u} dF + \int_V \mathbf{R}_V \cdot \delta\mathbf{u} dV + \int_V sn\rho_w g \cdot \delta\mathbf{u} dV, \tag{4}$$

where $\delta\varepsilon$ is the virtual strain rate, $\delta\mathbf{u}$ is the virtual displacement, $\mathbf{R}_F$ is the surface force per unit area, $\mathbf{R}_V$ is the volume force per unit volume (the weight of the liquid is not included), ρ_w is the mass density of the liquid, g is the gravitational acceleration (it is assumed to be a constant and to act in the constant direction), s is the degree of saturation, and n is the porosity of the medium.

Equation (4) is the governmental equation for finite element analysis in unsaturated soils.

3. Material Parameters in Unsaturated Soils and Shear Strength Reduction Method

3.1. Permeability and Degree of Saturation. The constitutive behavior for pore fluid flow in unsaturated soils is generally governed either by Darcy's law or by Forchheimer's law. Darcy's law can be considered to be a linearized version of Forchheimer's law.

According to Forchheimer's law, the negative gradient of the piezometric head is related to a quadratic function of the volumetric flow rate of the wetting liquid through a unit area of the medium [11]:

$$sn\mathbf{v}_w \left(1 + \beta\sqrt{\mathbf{v}_w \cdot \mathbf{v}_w}\right) = -\widehat{k} \cdot \frac{\partial \Phi}{\partial \mathbf{x}}, \tag{5}$$

where $\widehat{k}$ is the permeability of the medium and Φ is the piezometric head defined as follows:

$$\Phi = z + \frac{u_w}{g\rho_w}, \tag{6}$$

where z is the elevation above some datum plane, g is the magnitude of the gravitational acceleration, which acts in the direction opposite to z, $\mathbf{v}_w$ is the fluid velocity, and β is a "velocity coefficient" [12].

If $\beta = 0$, Forchheimer's law and Darcy's law are identical.

$\widehat{k}$ can be anisotropic and is a function of the degree of saturation and the void ratio of the medium. Some researchers referred to $\widehat{k}$ as the hydraulic conductivity $\mathbf{K}$ and defined the permeability as follows [13]:

$$\mathbf{K} = \frac{\nu}{g} \frac{1}{\left(1 + \beta\sqrt{\mathbf{v}_w \cdot \mathbf{v}_w}\right)} \widehat{k}, \tag{7}$$

where ν is the ratio of the fluid's dynamic viscosity to its density (the kinematic viscosity of the fluid).

If g is constant in magnitude and direction, the following equation can be obtained:

$$\frac{\partial \Phi}{\partial \mathbf{x}} = \frac{1}{g\rho_w} \left(\frac{\partial u_w}{\partial \mathbf{x}} - \rho_w \mathbf{g}\right), \tag{8}$$

where $\mathbf{g} = -g\ \partial z/\partial \mathbf{x}$ is the gravitational acceleration.

The permeability of a particular fluid in unsaturated soils depends on the degree of saturation of the considered phase and the porosity of the soils in ABAQUS program.

It can be assumed that the permeability in unsaturated soils is a function of the degree of saturation as follows:

$$\widehat{k} = k_s \mathbf{k}, \tag{9}$$

where $\mathbf{k}$ is the permeability of the fully saturated soils and k_s is the relative permeability depending on the degree of saturation.

In the fully coupled seepage-stress analysis, stress changes will affect the void ratio, and void ratio changes will in turn affect the permeability of the fully saturated soil. It can be assumed that volume strain is, in most cases, caused by the changes of pore volume. Therefore, the permeability of the fully saturated soil is represented by the stress tensor as the following equation because the void ratio is a function of the volume strain and the volume strain is a function of the stress tensor.

$$\mathbf{k} = f(\boldsymbol{\sigma}). \tag{10}$$

The permeability changes of the fully saturated soil due to the changes of the void ratio can be determined from the soil experiments. If there is a lack of the experimental data, the empirical formula can be used.

While, in the fully saturated soils, $k_s = 1.0$. Nguyen and Durso [14] observed that the permeability varies with s^3 (s is the degree of saturation) in steady flow through a partially saturated medium. Therefore, it can be assumed that $k_s = s^3$. If s is equal to the effective saturation, it can be expressed as following with the unsaturated parameters α and n [15]:

$$s = \left[1 + \left(\frac{\alpha u_w}{\gamma_w}\right)^n\right]^{-m}, \tag{11}$$

where $m = 1 - 1/n$ and γ_w is the volume weight of wetting liquid.

The degree of saturation is within a certain limited range, and typical forms of this limited range are shown in Figure 1 [14].

The wetting liquid is assumed to be contained always in the medium, i.e., $s > 0$.

Bear [13] showed that the transition between absorption and exsorption and vice versa takes place along "scanning" curves. This is approximated with a straight line, as shown in Figure 1.

3.2. Shear Strength in Unsaturated Soils and Shear Strength Reduction Method. Vanapalli et al. [16] suggested the following equation to determinate the shear strength in unsaturated soils.

$$\tau_f = c + (\sigma_n - u_a)\tan\varphi + (u_a - u_w)\left[(\tan\varphi)\left(\frac{\theta_w - \theta_r}{\theta_s - \theta_r}\right)\right], \tag{12}$$

where τ_f is the shear strength in unsaturated soils, c is the effective cohesion in unsaturated soils, $(\sigma_n - u_a)$ is the net normal stress, and σ_n is the total normal stress. $(u_a - u_w)$ is the matric suction, and φ is the effective friction angle with respect to net normal stress for a saturated soil. θ_w is the

volumetric water content, θ_s is the saturated volumetric water content, and θ_r is the residual volumetric water content.

The friction angle φ^b corresponding to the matric suction is assumed as follows:

$$\begin{aligned}\tan\varphi^b &= (\tan\varphi)s_e \\ &= (\tan\varphi)\left(\frac{\theta_w-\theta_r}{\theta_s-\theta_r}\right),\end{aligned} \tag{13}$$

where s_e is the effective saturation and it is determined from the soil-water characteristic curve.

Then, equation (12) expressing the shear strength of unsaturated soils can be expressed as follows [17, 18]:

$$\tau_f = c + (\sigma_n - u_a)\tan\varphi + (u_a - u_w)\tan\varphi^b. \tag{14}$$

If the pore gas is exposed to the atmosphere, then $u_a = 0$ in equation (14).

When $c' = c - u_w\tan\varphi^b$ and $\varphi' = \varphi$ in here, the following equation can be written:

$$\tau_f = c' + \sigma_n\tan\varphi'. \tag{15}$$

In the shear strength reduction FEM, the meaning of the safety factor of slopes is identical to that in the conventional limit equilibrium methods.

The reduced strength parameters are expressed as follows [17, 19]:

$$\begin{aligned}c_f &= \frac{c'}{F_t}, \quad \phi_f \\ &= \arctan\left(\frac{\tan\phi'}{F_t}\right),\end{aligned} \tag{16}$$

where c_f and ϕ_f are, respectively, the reduced cohesion and the reduced friction angle, c' and ϕ' are, respectively, the cohesion and the friction angle, and F_t is the shear strength reduction factor.

To determine the safety factor of ERD using the relations described above, first, the coupled seepage-stress finite element analysis is performed by ABAQUS-6.14 program, and a relationship curve between horizontal displacement and reduction factor is plotted at a certain position on the upstream slope. Then, the safety factor is obtained by finding a point of inflection on the relationship curve between horizontal displacement and reduction factor.

4. The Stability Reduction Characteristics of ERDs under RDD

4.1. The Schematic Cross Sections of ERDs, Material Parameters, and Analysis Cases. Prior to analysis, the drawdown ratio is assumed as follows:

$$r = \frac{\Delta H}{H}, \tag{17}$$

where r represents the drawdown ratio, H is the initial water level, and ΔH is the final drop of the external water level (Figure 2).

The drawdown rate is assumed as follows:

$$v_R = \frac{\Delta H}{t}, \tag{18}$$

where v_R represents the drawdown rate, t is the time of drawdown, and ΔH is the final drop of the external water level.

If the parameters of materials, the drawdown ratio, and the drawdown rate are, respectively, the same in the ERDs, the stability variation characteristics of the dams during RDD will be related to the gradient of the slopes.

To compare the sliding stability reduction characteristics of typical dams during RDD, the analysis was performed under the following conditions:

(i) The case that the corresponding slopes of the ERDs have the same gradients (Figure 3)

(ii) The case that the steady safety factors of upstream slopes are equal in the magnitude (but the corresponding slopes are not equal in the gradient), as shown in Figure 4

Figure 3 shows the schematic cross sections of ERDs for the case of the same slope gradients, while Figure 4 shows the sections for the case of the same steady safety factors on the upstream slopes. In the central core dam (CCD) or the sloping upstream core dam (SUCD), the cores have the suitable thicknesses so that the lengths of the seepage path through them are possibly the same. In all the cross sections, the height of the ERDs is 26m, and the initial water level is 24m on the upstream side. The ERDs have the horizontal drains with the length of 15m on the downstream side.

The ERDs are composed of the homogeneous and isotropic soils.

Tables 1 and 2 show the physicomechanical and the permeability parameters of the soils in the ERDs, respectively. With the use of unsaturated parameters α and n in Table 2, the relationship between the pore water pressure and the degree of saturation is obtained according to equation (11) during the performance.

In these analyses, three ERDs with two different drawdown ratios (i.e., 0.415 and 0.830) and three different drawdown rates (i.e., 0.1 m/d, 0.5 m/d, and 1.0 m/d) were considered. The drawdown ratio of $r = 0.415$ means that the reservoir water level drops from 24 m to 14 m, and $r = 0.830$ means that the reservoir water level drops from 24m to 4m.

The water level variation with time is modeled using the User Subroutine DISP in ABAQUS program. The framework of the User Subroutine DISP is shown in Appendix. U in the User Subroutine is the pore water pressure representing the reservoir water level, TIME is an array variable representing the time, and COORDS is an array variable containing the current coordinates. In this program, the reservoir water level variation is simulated by setting the pore water pressure into the variable U(1) during RDD.

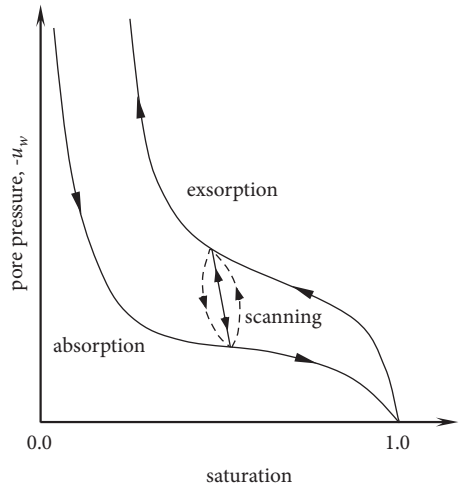

Figure 1: Typical absorption and exsorption behavior in unsaturated soils.

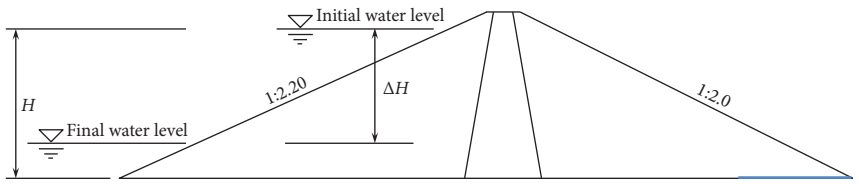

Figure 2: The final drop of external water level.

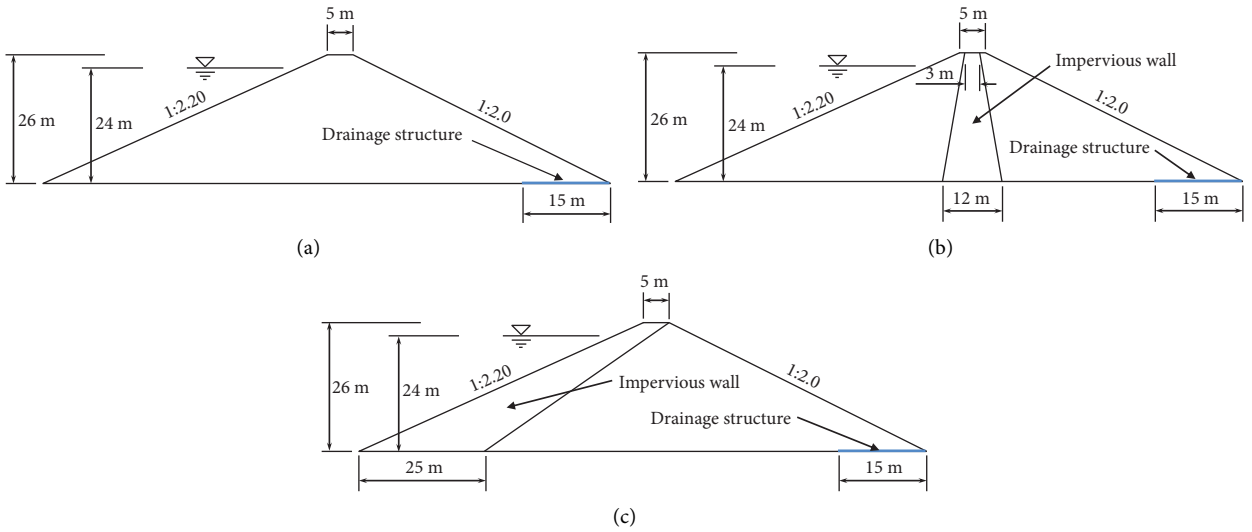

Figure 3: The schematic cross sections in the case of the same slope gradients: (a) homogeneous dam, (b) CCD, and (c) SUCD.

The stability of the slopes was analyzed by using the shear strength reduction method with ABAQUS-6.14. The element type of CPE4P was also used in the analysis, and elements of about 500 were taken in each ERD.

The effects of the mesh on the stability of ERDs do not be considered in the present work because a relationship curve between horizontal displacement and reduction factor is employed in order to obtain the safety factor of ERDs. The results of finite element analysis affect the mesh and especially stress and strain. But it seems that the effects of the mesh on the displacement are not large so that the position of the inflection point on the relationship curve between horizontal displacement and reduction factor is almost unchanged depending on the mesh.

4.2. The Stability Reduction Characteristics. The stability matter of the ERDs during RDD is ascribable to a stability

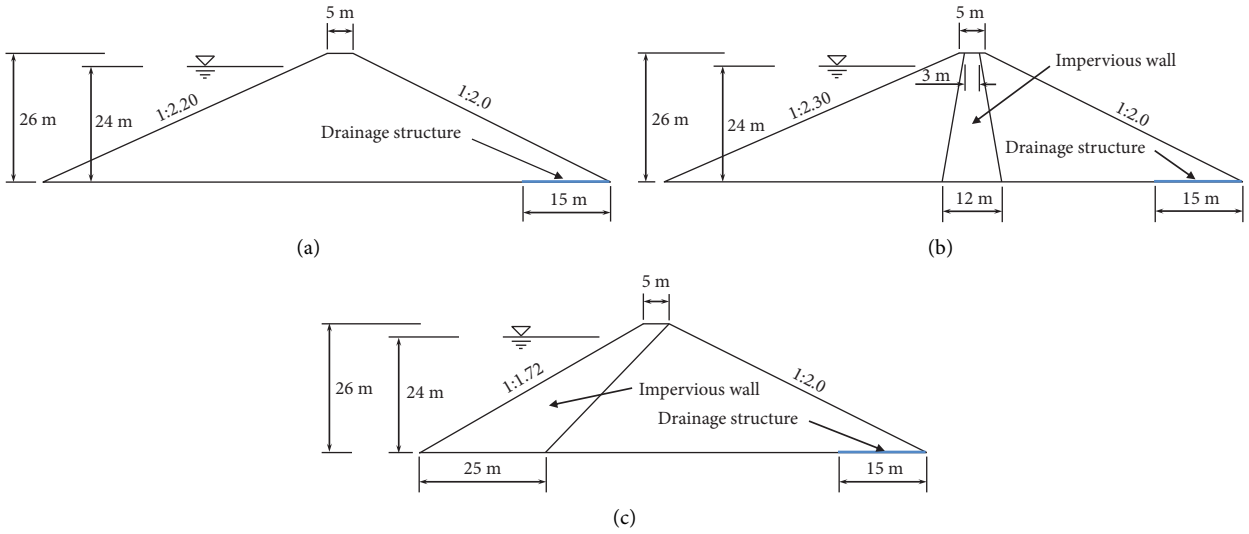

Figure 4: The schematic cross sections in the case of the same steady safety factors on the upstream slopes: (a) homogeneous dam, (b) CCD, and (c) SUCD.

Table 1: Physicomechanical parameters of soils.

Material name		Density ρ kg/m^3	Young's modulus E MPa	Poisson's ratio ν	Cohesion c kPa	Friction angle φ °
Shell	Sandy soil	2050	52	0.30	4	33
Impervious core	Sandy clay	1800	18	0.35	16	16

Table 2: Permeability parameters of soils.

Material name		Void ratio e	Permeability **k** m/s	Unsaturated parameters α m^{-1}	n	Residual volumetric water content θ_r	Saturated volumetric water content θ_s
Shell	Sandy soil	1.0 1.5	10^{-5} 10^{-4}	7.5	1.89	0.057	0.41
Impervious core	Sandy clay	1.0 1.5	10^{-7} 10^{-6}	0.8	1.09	0.095	0.41

question of the upstream slopes. Therefore, the upstream slopes were considered only in the present work for the study of stability variation characteristic.

4.2.1. In the Case of the Same Slope Gradients. In three ERDs, the gradient is 1V:2.20H on the upstream slope and is 1V:2.0H on the downstream slope.

Figures 5–7 show the stability variation versus time for the upstream slopes of the ERDs. The obtained results represent that the smaller the drawdown rate is, the more the stability variation curves have the gentler gradients, and it takes a longer time to reach a minimum safety factor. A minimum safety factor occurs generally at a time of the minimum water level of the reservoir. For example, in three ERDs with the drawdown ratio of 0.830, the minimum safety factors occur, respectively, at the time of 480 hours for the drawdown rate v_R = 1.0m/d, at the time of 960 hours for v_R = 0.5m/d and at the time of 4,800 hours for v_R = 0.1m/d.

In three ERDs with a drawdown ratio of 0.415, the minimum safety factors occur, respectively, at the time of 240 hours for the drawdown rate v_R = 1.0m/d, at the time of 480 hours for v_R = 0.5m/d and at the time of 2,400 hours for v_R = 0.1m/d. The reason seems that the effects of the water pressure supporting the upstream slopes reach the minimum but the effects of the pore water pressure inducing the sliding failure reach the maximum when the water level of the reservoir comes to the lowest level.

The results show that the decrement of the safety factor in the SUCDs is larger than that of the CCD or the homogeneous dam. And after arriving at the safety factor of minimum, the stability of the SUCD does not increase so clearly as that of the CCD or the homogeneous dam (Figure 7). The reason seems to be that the degree of saturation

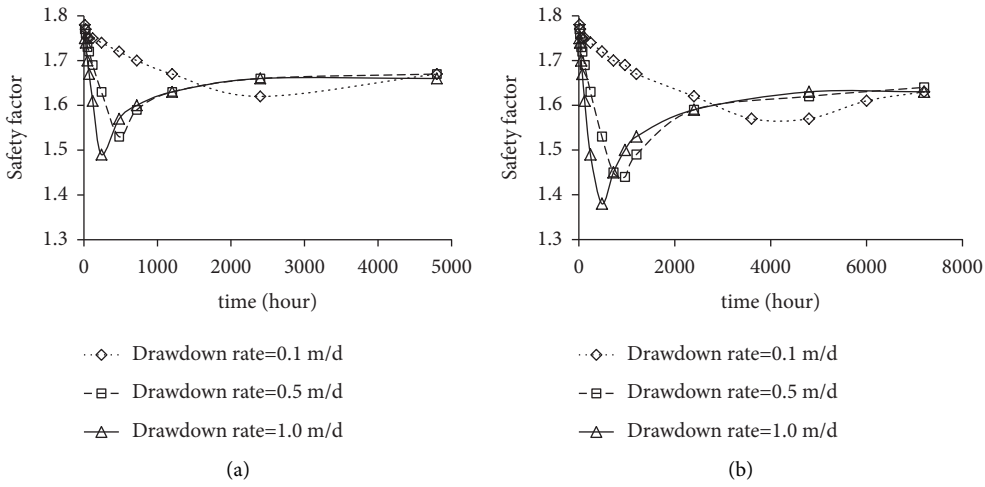

Figure 5: The stability variation versus time in the homogeneous dams (with the same slope gradients): (a) $r = 0.415$ and (b) $r = 0.830$.

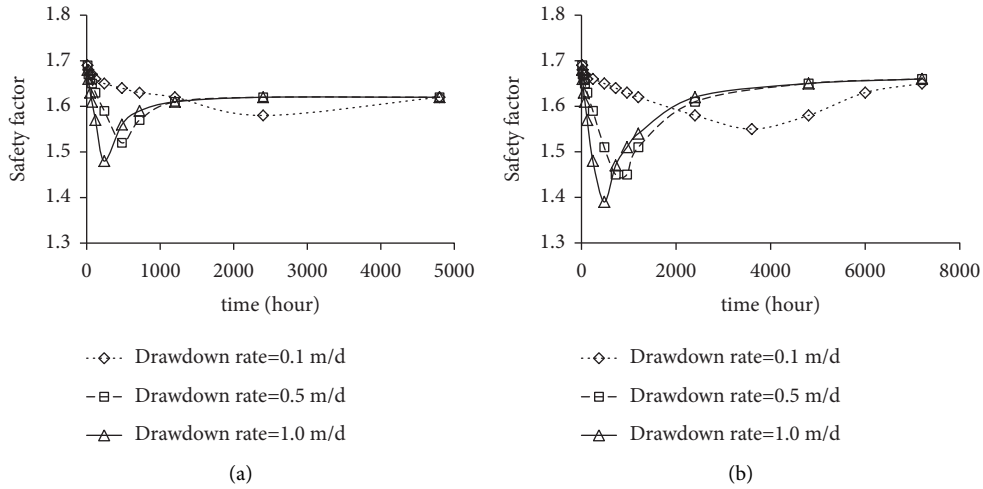

Figure 6: The stability variation versus time in the CCDs (with the same slope gradients): (a) $r = 0.415$ and (b) $r = 0.830$.

does not significantly decrease in the impervious material of the upstream slope of the SUCD after the drop of the external water level. For example, Figure 8 shows the saturation variation versus time in the impervious core of the upstream slope after 960 hours (the time for the lowest water level) when $r = 0.830$ and $v_R = 0.5$m/d; that is, although it passes the long period after the safety factor arrives at the minimum, the degree of saturation does not decrease to below 0.75, and its space distribution also has no significant variation. But the degree of saturation drops to about zero in a short time after 960 hours (the time for the lowest water level) in the CCD or the homogeneous dam (Figure 9). These results show that the decrease of the stability is easy, but the restoration of the original stability is very hard in the SUCD under RDD.

Table 3 shows the steady safety factors, the minimum safety factors, the decrements, and the decreasing rates in the typical ERDs under RDD. In Table 3, the decrements are obtained by subtracting the minimum safety factor from the steady safety factor, and the decreasing rates are defined as follows:

$$R_{sf} = \frac{F_s - F_{\min}}{F_s}, \tag{19}$$

where R_{sf} is the decreasing rate of the safety factor, F_s is the steady safety factor, and $F_{\min}$ is the minimum safety factor obtained from the stability variation versus time for the upstream slopes.

It is clear that decrements and decreasing rates of the safety factors increase with an increase in the drawdown ratio and the drawdown rate in the identical type of ERD. This allows us to take the new opinion that the smaller the drawdown ratio and the drawdown rate are, the safer the upstream slopes of dams can be under RDD.

When the variation characteristic of the sliding stability for typical ERDs is considered under the same situations of

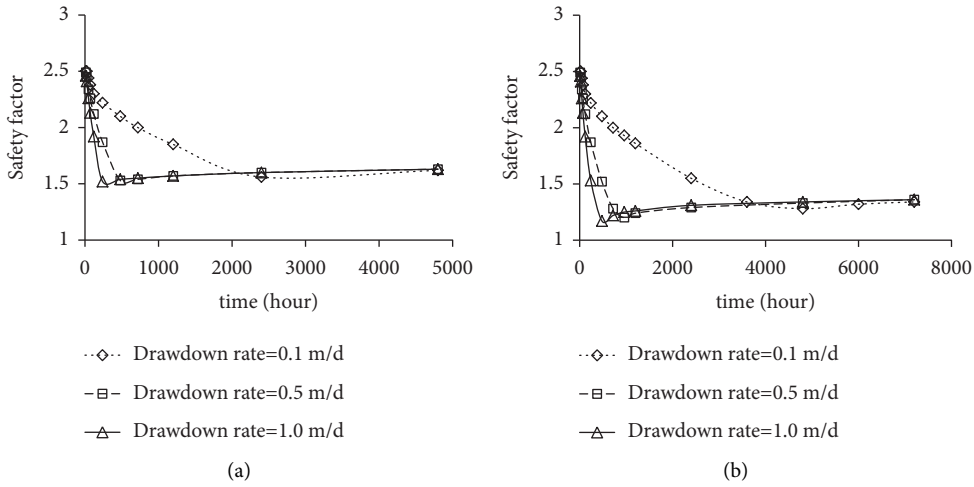

Figure 7: The stability variation versus time in the SUCDs (with the same slope gradients): (a) $r = 0.415$ and (b) $r = 0.830$.

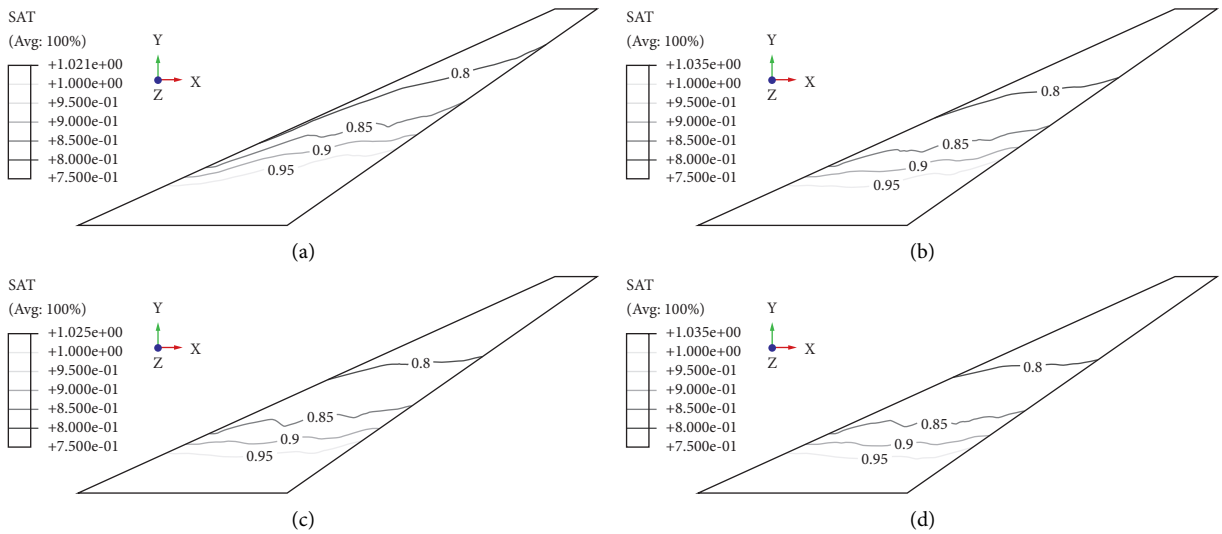

Figure 8: The saturation distribution variation versus time in the impervious core of the SUCD: (a) 1,200h, (b) 2,400h, (c) 4,800h, and (d) 7,200h.

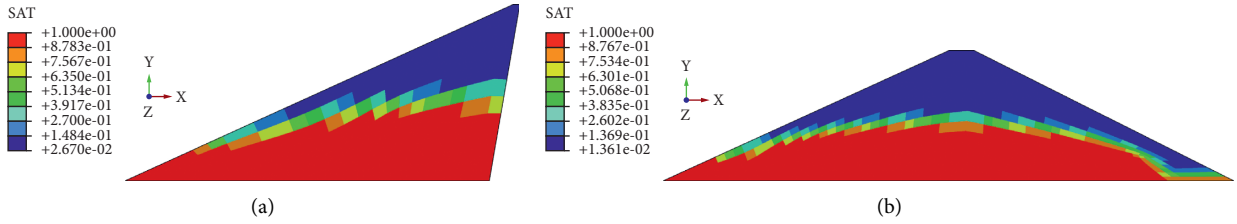

Figure 9: The saturation distribution at 1,200 hours: (a) the CCD and (b) the homogeneous dam.

the drawdown ratio and the drawdown rate, the safe type of ERD can be found under the RDD. From comparison to the decrements of safety factors in typical ERDs under the same situations of the drawdown ratio and the drawdown rate, the CCDs have the smallest decrement, while the SUCDs have the largest decrement.

Meanwhile, the decreasing rates of safety factors are also smallest in the CCDs while are largest in the SUCDs. For example, when $r = 0.830$ and $v_R = 0.5$m/d, the decrement of the safety factor is 0.23, and the decreasing rate of the safety factor is 0.1369 for the CCD while the decrement of the safety factor is 1.02 which is relatively large for the SUCD.

Table 3: The stability estimation on the upstream slopes of ERDs (with the same slope gradients).

Drawdown ratio r	Drawdown rate v_R	Safety factor											
		Homogeneous dam				CCD				SUCD			
		Steady F_s	Minimum $F_{\min}$	Decrement $F_s - F_{\min}$	Decreasing rate R_{sf}	Steady F_s	Minimum $F_{\min}$	Decrement $F_s - F_{\min}$	Decreasing rate R_{sf}	Steady F_s	Minimum $F_{\min}$	Decrement $F_s - F_{\min}$	Decreasing rate R_{sf}
0.415	0.1	1.75	1.62	0.13	0.0743	1.68	1.58	0.10	0.0595	2.22	1.56	0.66	0.2973
	0.5	1.75	1.53	0.22	0.1257	1.68	1.52	0.16	0.0952	2.22	1.53	0.69	0.3108
	1.0	1.75	1.49	0.26	0.1486	1.68	1.48	0.20	0.1190	2.22	1.52	0.70	0.3153
0.830	0.1	1.75	1.57	0.18	0.1029	1.68	1.55	0.13	0.0774	2.22	1.28	0.94	0.4234
	0.5	1.75	1.44	0.31	0.1771	1.68	1.45	0.23	0.1369	2.22	1.20	1.02	0.4595
	1.0	1.75	1.38	0.37	0.2114	1.68	1.39	0.29	0.1726	2.22	1.17	1.05	0.4730

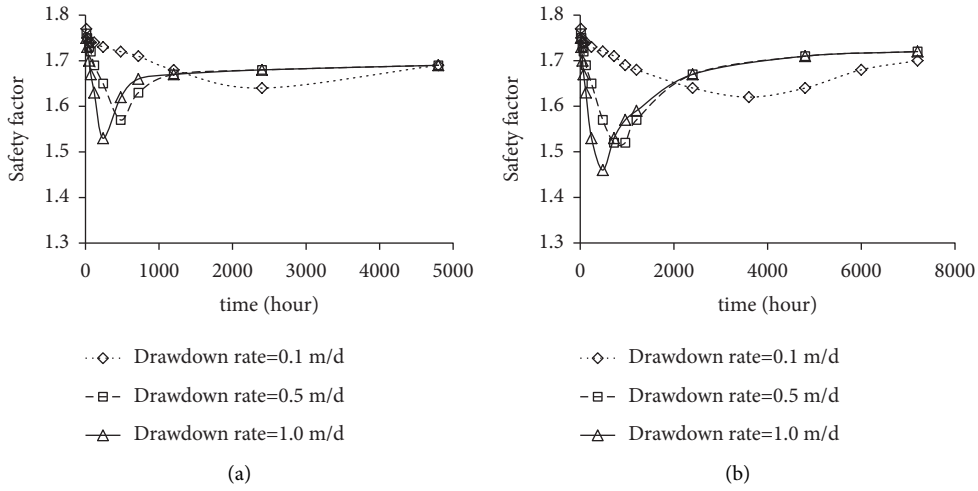

Figure 10: The stability variation versus time in the CCDs (with the same steady safety factors on the upstream slopes): (a) $r = 0.415$ and (b) $r = 0.830$.

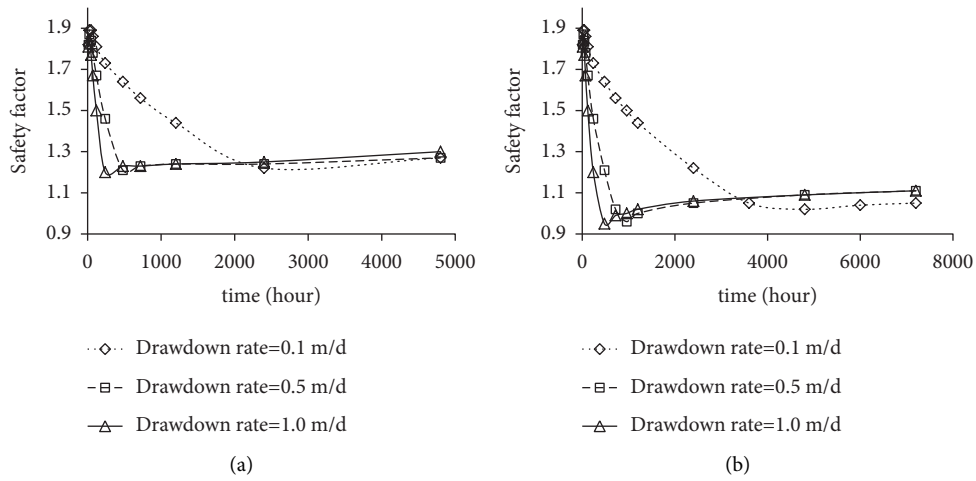

Figure 11: The stability variation versus time in the SUCDs (with the same steady safety factors on the upstream slopes): (a) $r = 0.415$ and (b) $r = 0.830$.

Here, the decreasing rate of the safety factor is 0.4595 for the SUCD and is about 3.4 times that for the CCD about 2.6 times that for the homogeneous dam.

4.2.2. In the Case of the Same Steady Safety Factors on the Upstream Slopes. The steady safety factors are, respectively, 1.75 at the upstream slope gradient of 1V:2.20H for the homogeneous dam, at the gradient of 1V:2.30H for the CCD, and at the gradient of 1V:1.72H for the SUCD.

In these cases, the stability reduction characteristic of the typical ERDs was studied under RDD. Figures 10 and 11 show the stability variation versus time in the CCDs and the SUCDs, respectively, while the stability variation versus time for the homogeneous dams is already shown in Figure 5.

Table 4 shows the steady safety factors, the minimum safety factors, the decrements, and decreasing rates of the safety factors. Table and figures also represent that the smaller the drawdown rate is, the gentler the gradients of stability variation curves are, and it takes a longer time to reach a minimum of the safety factor.

The results also show that the decrements and decreasing rates of the safety factors in the SUCD are greater than these of the CCD or the homogeneous dam. The CCDs have smallest decrements of the safety factors, while the SUCDs have largest decrements of the safety factors under the same situations of the drawdown ratio and the drawdown rate.

The characteristic of the stability variation curves is also agreed with the above case (case with the same slope gradients) of typical ERDs.

Table 4: The stability estimation on the upstream slopes of ERDs (with the same steady safety factors on the upstream slopes).

Drawdown ratio r	Drawdown rate v_R	Safety factor											
		Homogeneous dam				CCD				SUCD			
		Steady F_s	Minimum $F_{\min}$	Decrement $F_s - F_{\min}$	Decreasing rate R_{sf}	Steady F_s	Minimum $F_{\min}$	Decrement $F_s - F_{\min}$	Decreasing rate R_{sf}	Steady F_s	Minimum $F_{\min}$	Decrement $F_s - F_{\min}$	Decreasing rate R_{sf}
0.415	0.1	1.75	1.62	0.13	0.0743	1.75	1.64	0.11	0.0629	1.75	1.22	0.53	0.3029
	0.5	1.75	1.53	0.22	0.1257	1.75	1.57	0.18	0.1029	1.75	1.21	0.54	0.3086
	1.0	1.75	1.49	0.26	0.1486	1.75	1.53	0.22	0.1257	1.75	1.20	0.55	0.3143
0.830	0.1	1.75	1.57	0.18	0.1029	1.75	1.62	0.13	0.0743	1.75	1.02	0.73	0.4171
	0.5	1.75	1.44	0.31	0.1771	1.75	1.52	0.23	0.1314	1.75	0.96	0.79	0.4514
	1.0	1.75	1.38	0.37	0.2114	1.75	1.46	0.29	0.1657	1.75	0.95	0.80	0.4571

5. Conclusion

The results in this study have demonstrated a significant opinion that the CCD is safer than the other type of ERDs in the same condition for RDD. It has indicated that the steady stability of the SUCD is the highest one if it is compared with the remaining ERDs in the case of the same slope gradients. But Tables 3 and 4 show that the SUCDs are more unstable than the other type of ERDs in the RDD condition.

The results will be used for two purposes. First, it will help to select the type of ERD for the reservoir construction. In the embankments such as the reservoir dam of relatively small storage capacity than its height, the embankment under the effects of the high tide and the ebb tide, and the dam of agricultural reservoir, etc., it may be recommended to select the type of CCD to improve the stability of ERD for RDD. Meanwhile, in the embankments such as the reservoir dam of relatively large storage capacity than its height, the embankment of gentle water level variation, etc., the type of ERD which has larger steady stability for the same slope gradients is economically better, and the type of SUCD can be recommended. Second, the minimum safety factor for RDD may be approximately estimated by the types of ERD, the steady safety factor, the drawdown ratio, and the drawdown rate.

Appendix

The framework of the User Subroutine DISP is as follows:

```
SUBROUTINE DISP(U,KSTEP, KINC,TIME, NODE,
NOEL, JDOF,COORDS)
C
INCLUDE''ABA_PARAM.INC''
C
DIMENSION U(3),TIME(2),COORDS(3)
C
user coding to define U
END
```

Data Availability

The data used to support the findings of this study are available from the corresponding author upon request.

Conflicts of Interest

The authors declare that they have no conflicts of interest regarding the publication of this study.

Acknowledgments

This study was financially supported by the Scientific and Technological Advance of DPR Korea (Grant no. 24-2020-730621).

References

[1] M. Huang and C.-Q. Jia, "Strength reduction FEM in stability analysis of soil slopes subjected to transient unsaturated seepage," *Computers and Geotechnics*, vol. 36, no. 1-2, pp. 93–101, 2009.

[2] M. M. Berilgen, "Investigation of stability of slopes under drawdown conditions," *Computers and Geotechnics*, vol. 34, no. 2, pp. 81–91, 2007.

[3] R. Khanna, M. Datta, and G. V. Ramana, "Influence of core thickness on stability of upstream slope of earth and rockfill dams under rapid-draw-down," in *Proceedings of the 50th Indian Geotechnical Conference*, pp. 17–19, Pune, Maharashtra, India, December 2015.

[4] A. H. Boushehrian, A. Rezaee, and A. Vafamand, "Studying the effect of horizontal drains on stability of heterogeneous and homogeneous earth dams during rapid drawdown condition," *Journal of Structural Engineering and Geotechnics*, vol. 7, no. 1, pp. 31–45, 2017.

[5] A. Tsiampousi, L. Zdravković, and D. M. Potts, "Variation with time of the factor of safety of slopes excavated in unsaturated soils," *Computers and Geotechnics*, vol. 48, pp. 167–178, 2013.

[6] N. M. Pinyol, E. E. Alonso, and S. Olivella, "Rapid drawdown in slopes and embankments," *Water Resources Research*, vol. 44, pp. 1–22, 2008.

[7] X. P. Chen and J. W. Huang, "Stability analysis of bank slope under conditions of reservoir impounding and rapid drawdown," *Journal of Rock Mechanics and Geotechnical Engineering*, vol. 3, no. Supply, pp. 429–437, 2011.

[8] T. D. Stark and N. H. Jafari, "Rapid Drawdown Stability Analysis of San Luis Dam," in *Proceedings of the 3rd North American Symposium on Landslides*, pp. 1–8, Roanoke, VA, USA, June 2017.

[9] H. Keykhah and B. D. Zadeh, "Stability analysis of upstream slope of earthen dams using the finite element method against sudden variation in the water surface of the reservoir, case study: Ilam Earthen Dam in Ilam Province," *Journal of Civil Engineering and Materials Application*, vol. 2, no. 1, pp. 24–30, 2018.

[10] T. H. Wu, *Soil Mechanics*, Allyn & Bacon, Boston, 1976.

[11] C. S. Desai, "Finite element methods for flow in porous media," in *Finite Elements in Fluids*, pp. 157–181, Wiley, Hoboken, NJ, USA, 1975.

[12] S. M. Tariq, "Evaluation of flow characteristics of perforations including nonlinear effects with the finite-element method," *SPE Production Engineering*, vol. 2, no. 2, pp. 104–112, 1987.

[13] J. Bear, *Dynamics of Fluids in Porous media*, American Elsevier Publishing Company, Dover, New York, NY, USA, 1972.

[14] H. V. Nguyen and D. F. Durso, "Absorption of water by fiber webs: an illustration of diffusion transport," *Tappi Journal*, vol. 66, no. 12, 1983.

[15] M. T. van Genuchten, "A closed-form equation for predicting the hydraulic conductivity of unsaturated soils," *Soil Science Society of America Journal*, vol. 44, no. 5, pp. 892–898, 1980.

[16] S. K. Vanapalli, D. G. Fredlund, D. E. Pufahl, and A. W. Clifton, "Model for the prediction of shear strength with respect to soil suction," *Canadian Geotechnical Journal*, vol. 33, no. 3, pp. 379–392, 1996.

[17] F. Cai, K. Ugai, A. Wakai, and Q. Li, "Effects of horizontal drains on slope stability under rainfall by three-dimensional

finite element analysis," *Computers and Geotechnics*, vol. 23, no. 4, pp. 255–275, 1998.

[18] J. M. Gasmo, H. Rahardjo, and E. C. Leong, "Infiltration effects on stability of a residual soil slope," *Computers and Geotechnics*, vol. 26, no. 2, pp. 145–165, 2000.

[19] F. Cai and K. Ugai, "Numerical analysis of rainfall effects on slope stability," *International Journal of Geomechanics*, vol. 4, no. 2, pp. 69–78, 2004.